

## Domain growth in the three-dimensional random-field Ising magnet $\text{Fe}_{0.5}\text{Zn}_{0.5}\text{F}_2$

Q. Feng and R. J. Birgeneau

*Department of Physics, Massachusetts Institute of Technology, Cambridge, Massachusetts 02139*

J. P. Hill

*Department of Physics, Brookhaven National Laboratory, Upton, New York 11973*

(Received 12 January 1995)

Complementary neutron-scattering and superconducting quantum interference device (SQUID) magnetometry measurements have been carried out to study the time dependence of the field-cooled metastable domains in  $\text{Fe}_{0.5}\text{Zn}_{0.5}\text{F}_2$ . These neutron-scattering data provide direct evidence of a logarithmic increase in the correlation length upon quenching the system to  $T \leq T_c$  at  $H = 5.5$  T. At low temperatures the magnetic domains are frozen on experimental time scales. SQUID measurements performed at a series of fields and temperatures confirm the evolution of the excess magnetization  $M_{\text{ex}}$  arising from domain surfaces and allow quantitative analysis of its time dependence. Specifically, we found that  $M_{\text{ex}} \sim H^{\nu_M} [\ln(t/\tau)]^{-\psi}$ , where  $\nu_M = 2.7 \pm 0.1$  and  $\psi = 1.1 \pm 0.3$  for  $H \geq 3.45$  T;  $\psi$  is much less than 1 for lower fields. In particular,  $\psi = 0.42 \pm 0.14$  at  $H = 1.5$  T, in agreement with a prediction by Nattermann and Vilfan. At  $H = 5.5$  T,  $M_{\text{ex}}(T)$  and the inverse correlation length  $\kappa(T)$  exhibit identical time dependences. Overall, these measurements reveal the varied time dependence of a field-cooled, strongly anisotropic dilute antiferromagnet in different applied fields, and shed light on the mechanisms of domain evolution.

### I. INTRODUCTION

The random-field Ising model (RFIM), as a system with disorder and competing interactions, has attracted much interest since the 1970's. Studies on systems modeled by the RFIM have displayed a variety of intriguing phenomena including especially rich dynamical behavior.<sup>1,2</sup> Early theoretical work focused on the lower critical dimension of the RFIM. Following a heuristic argument by Imry and Ma<sup>3</sup> and later a rigorous proof by Imbrie,<sup>4</sup> a RFIM system in thermal equilibrium is expected to achieve long-range order (LRO) in dimensions greater than 2. On the experimental front, most work has been done on various diluted antiferromagnets in uniform applied fields (DAFF) after this Hamiltonian was mapped onto that of the RFIM by Fishman and Aharony<sup>5</sup> and Cardy.<sup>6</sup> Although experiments performed on 2d and 3d DAFF's were expected to determine unambiguously the lower critical dimension of the RFIM, the interpretation of the results was obscured by the presence of strong hysteresis in the 3d DAFF's.<sup>1</sup> Early neutron-scattering experiments on  $\text{Fe}_{0.7}\text{Mg}_{0.3}\text{Cl}_2$  by Wong and Cable found hysteretic behavior in the scattering intensity following different paths in the  $H$ - $T$  plane.<sup>7</sup> They interpreted this as a result of the existence of a domain phase. Cowley *et al.* carried out a more careful study on randomly diluted  $\text{Fe}_x\text{Zn}_{1-x}\text{F}_2$ .<sup>8</sup> They confirmed that a short-range ordered (SRO) domain state was formed as the system was cooled in the presence of a random field (FC) or field lowered at a constant temperature across the phase boundary. The size of these domains was measured as a function of temperature and applied field. On

the other hand, if the system was cooled to a low temperature below the Néel temperature ( $T_N$ ) in zero field and a field was subsequently applied [a procedure known as zero-field cooling (ZFC)], it retained LRO until it was warmed through the transition. Related hysteresis effects were observed by Shapira, Oliveira, and Foner in  $\text{Mn}_{0.75}\text{Zn}_{0.25}\text{F}_2$  using various bulk thermodynamic techniques.<sup>9</sup>

Following the experimental discoveries, theoretical work indicated that the anomalously slow dynamics in the RFIM causes its true equilibrium behavior to evade investigation on experimental time scales.<sup>10,11</sup> As a 3d RFIM system is cooled through the transition from the disordered paramagnetic phase, it falls out of equilibrium into a metastable domain state.<sup>12,13</sup> The structure of the FC domains is determined by a competition between energy costs due to unsatisfied bonds between neighboring spins and gains due to random fields (RF) and random bonds (RB) in a DAFF. The metastability results from the presence of multiple minima in the free energy corresponding to differing spin configurations. For  $T < T_c(H)$ , where  $T_c(H)$  is a pseudocritical temperature associated with the ZFC *trompe l'oeil* phase boundary<sup>14</sup> and  $H$  is the applied uniform field that determines the strength of the quenched random fields, energy barriers  $\Delta E$  may be overcome through thermal activation on a time scale  $t \sim \exp(\Delta E/kT)$ , and the domains are expected to relax towards the LRO equilibrium state. For a RFIM system in the field-cooled state, Villain has argued that the dynamic lower critical dimension is 4 and that the domain relaxation time in three dimensions is infinite.<sup>12</sup> On general grounds, it is expected that the average size of these field-cooled domains grows logarithmically with time.<sup>12,15</sup>

An indication of such metastable effects has been observed by Wong and Cable<sup>7</sup> in their study on  $\text{Fe}_{0.7}\text{Mg}_{0.3}\text{Cl}_2$ , where the FC peak intensity showed a clear increase over a period of 6 h (though most of the change occurred within the first hour). No attempt was made to measure the time evolution of the domain size itself. A similar effort to study the time dependence of the FC domains in  $\text{Mn}_x\text{Zn}_{1-x}\text{F}_2$  by neutron scattering yielded negative results. In particular, Cowley *et al.*<sup>16</sup> carefully studied the FC domains in  $\text{Mn}_x\text{Zn}_{1-x}\text{F}_2$  at several fields and temperatures and did not discern any notable change in either the peak intensity or the domain size over two decades in time. However, optical Faraday rotation<sup>17,18</sup> and superconducting quantum interference device (SQUID) magnetometry<sup>19,20</sup> performed on  $\text{Fe}_x\text{Zn}_{1-x}\text{F}_2$  with various levels of dilution have shown the FC uniform magnetization  $M_{\text{FC}}$  to decay logarithmically over time. This has been interpreted as a manifestation of domain wall motion in the metastable state.

Following these apparently contradictory experimental results on the time dependence in  $3d$  DAFF's, Nattermann and Vilfan (NV) developed ideas stressing the role of broad and narrow domain walls and concluded that there was disparate time-dependent behavior for DAFF's with weak and strong anisotropy.<sup>21</sup> In systems with weak anisotropy and therefore broad domain walls, for example,  $\text{Mn}_{0.75}\text{Zn}_{0.25}\text{F}_2$  in which the dipolar anisotropy is only about 1% of the exchange energy, they predict that no domain relaxation should be observable within the usual experimental time scale of several hours. Conversely, NV predict that strongly anisotropic DAFF's with narrow domain walls should show a decaying uniform magnetization due to adjustments in the domain surfaces.  $\text{Fe}_x\text{Zn}_{1-x}\text{F}_2$  and  $\text{Fe}_x\text{Mg}_{1-x}\text{Cl}_2$  are examples of  $3d$  systems with strong anisotropy. The NV theory qualitatively describes the neutron-scattering findings in  $\text{Mn}_{0.75}\text{Zn}_{0.25}\text{F}_2$  and  $\text{Fe}_{0.7}\text{Mg}_{0.3}\text{Cl}_2$  and the magnetometry results in  $\text{Fe}_x\text{Zn}_{1-x}\text{F}_2$ . In their measurements on  $\text{Fe}_{0.46}\text{Zn}_{0.54}\text{F}_2$ , Lederman *et al.* mapped out the dynamic behavior in the  $H$ - $T$  plane based on systematic time dependence and field-cycling studies.<sup>22</sup> However, up to now, there has been no direct evidence of the predicted underlying domain evolution. The neutron-scattering experiment on  $\text{Fe}_{0.5}\text{Zn}_{0.5}\text{F}_2$  reported here was designed to study the metastable effects by directly measuring the correlation length in the FC state. We find a notable increase in the FC domain size for  $T \lesssim T_c(H)$ . No time dependence is observed at  $T = 6.8 \text{ K} \ll T_c(H)$  as a result of the frozen dynamics. This explains why domain relaxation was not detected in earlier experiments by Cowley *et al.* on a sample of the same composition.<sup>8</sup> In their experiment, the sample was quenched to low temperatures ( $T \approx 8 \text{ K}$ ). Our results are then compared with further SQUID magnetometry measurements of the uniform magnetization. At  $H = 5.5 \text{ T}$ , at several temperatures below  $T_c$  (5.5 T), the excess magnetization  $M_{\text{ex}} = M_{\text{FC}} - M_{\text{ZFC}}$  and the inverse correlation length,  $\kappa(T)$ , exhibit identical time dependences. Our findings are in support of the observations made by Lederman *et al.*<sup>22</sup> on the dynamics of  $3d$  DAFF's.

## II. EXPERIMENTAL PROCEDURE

The two  $\text{Fe}_{0.5}\text{Zn}_{0.5}\text{F}_2$  crystals used in these experiments were both obtained from the same  $20 \times 20 \times 10 \text{ mm}^3$  boule grown using the Czochralski method at MIT. The dimension of the samples were approximately  $10 \times 10 \times 3 \text{ mm}^3$  for the neutron scattering and  $6 \times 5 \times 2 \text{ mm}^3$  for the SQUID measurements, respectively. In both experiments, the samples were mounted with the  $c$  axis parallel to the vertical magnetic field to within  $5^\circ$ . Temperature stability was better than  $0.01 \text{ K}$ .

SQUID measurements show that the zero-field Néel temperature of  $\text{Fe}_{0.5}\text{Zn}_{0.5}\text{F}_2$  is  $T_N = 36.7 \text{ K}$ , which is close to  $0.5 \times T_N$  of pure  $\text{FeF}_2$ . Magnetic x-ray-scattering studies on a different sample of  $\text{Fe}_{0.5}\text{Zn}_{0.5}\text{F}_2$  from the same boule also yield  $T_N = 36.7 \text{ K}$ .<sup>23</sup> However,  $T_N$  determined by the neutron-scattering experiment is higher by  $3.1 \text{ K}$ . We believe that this discrepancy arises solely from an error in the magnet thermometer calibration in the neutron study, and throughout this paper, the neutron data have been shifted by  $\Delta T = -3.1 \text{ K}$ . The zero-field transition measured by neutron scattering shows a smearing that is less than  $0.1 \text{ K}$  [full width at half maximum (FWHM)], corresponding to a concentration gradient of less than  $0.1\%$  per mm. The crystal has a mosaic spread of  $0.01^\circ$  given by x-ray diffraction.

The neutron-scattering experiments were performed on spectrometer H7 at the High Flux Beam Reactor at Brookhaven National Laboratory. Measurements were carried out in the triple-axis mode. A PG(002) monochromator selected incident neutrons with an energy of  $14.7 \text{ meV}$ . The horizontal collimations were  $10'$ - $10'$ -sample- $10'$ - $80'$ . At the (100) reciprocal lattice point, this configuration gave rise to an in-plane resolution of  $0.0037 \text{ \AA}^{-1}$  full width at half maximum (FWHM) parallel to the momentum transfer,  $0.0014 \text{ \AA}^{-1}$  perpendicular to the momentum transfer and a  $0.088 \text{ \AA}^{-1}$  vertical resolution. The energy resolution was  $0.35 \text{ meV}$  FWHM.

In both experiments, the FC quenches begin with the system brought to equilibrium at  $10 \text{ K}$  above  $T_c(H)$  and then cooled rapidly through the transition to the target temperature in a constant field. Throughout this work, we define the ZFC critical temperature  $T_c(H)$  at an applied field,  $H$ , to be the temperature at which the ZFC critical scattering, or the temperature derivative of the uniform magnetization ( $dM/dT$ ) exhibits a peak.<sup>8,19</sup> The significance of such a definition of  $T_c(H)$  is further discussed by Hill and co-workers.<sup>14,24,25</sup> Time zero is taken to be the time at which the sample temperature crossed the metastability temperature  $T_M(H)$  associated with the phase boundary.<sup>24</sup> By definition, this is the point at which metastability is first established.<sup>19</sup> Immediately after the temperature is stabilized at the target value, transverse scans are taken repeatedly through the (100) peak in the neutron-scattering experiment, while in the SQUID measurements the uniform magnetization  $M$  is measured repeatedly. The time scales probed by both experiments are approximately 5 min to 5 h. Quenches to three different temperatures were taken at  $H = 5.5 \text{ T}$  during the neutron-scattering experiment and a variety of

fields and temperatures were studied in the SQUID measurements.

### III. NEUTRON-SCATTERING RESULTS

For the neutron-scattering portion of this work, FC quenches were performed at a fixed field  $H=5.5$  T [ $T_c(5.5\text{ T})=27.9$  K] to three temperatures below the phase boundary:  $T=6.8$ , 21.5, and 27.1 K. As we shall see, these temperatures represent three distinct regimes. No LRO component is observed in these measurements. The peak intensities for each of these temperatures are shown in Fig. 1. Over the time period studied, the (100) peak intensity is constant at  $T=6.8$  K, but increases notably at  $T=21.5$  and 27.1 K.

Before discussing these results further, we first present a brief outline of the data analysis techniques. The scattering amplitude near a magnetic reciprocal-lattice point  $\mathbf{G}$  is determined by the spin-spin correlation function of the  $z$  components  $\langle S_i^z S_j^z \rangle$  and, in the presence of a random field, is typically represented by the square of a Lorentzian<sup>8,26,27</sup>

$$S(\mathbf{Q}) = \frac{A\kappa}{[\kappa^2 + (q^*)^2]^2}, \quad (1)$$

where  $q^* = \mathbf{Q} - \mathbf{G}$  is expressed in reciprocal-lattice units. Written in this form,  $A$  is the integrated intensity and the correlation length is equal to  $1/\kappa$ . Transverse scans through (100) were fitted to Eq. (1) convolved with the instrumental resolution, plus a time-independent constant background, in order to determine the parameters  $A$  and  $\kappa$ . Such analysis of the data shows that  $\kappa$  decays significantly over a period of 5 h at  $T=21.5$  and 27.1 K, but remains constant to within the errors at  $T=6.8$  K. The fitted integrated intensity  $A$  remains constant over time for all temperatures.

However, although Eq. (1) provides excellent fits to the data at  $T=27.1$  K, systematic deviations from the data for large  $q^*$  at  $T=6.8$  and 21.5 K are seen. As shown in Fig. 2, the fit (dashed line) overestimates the intensity in

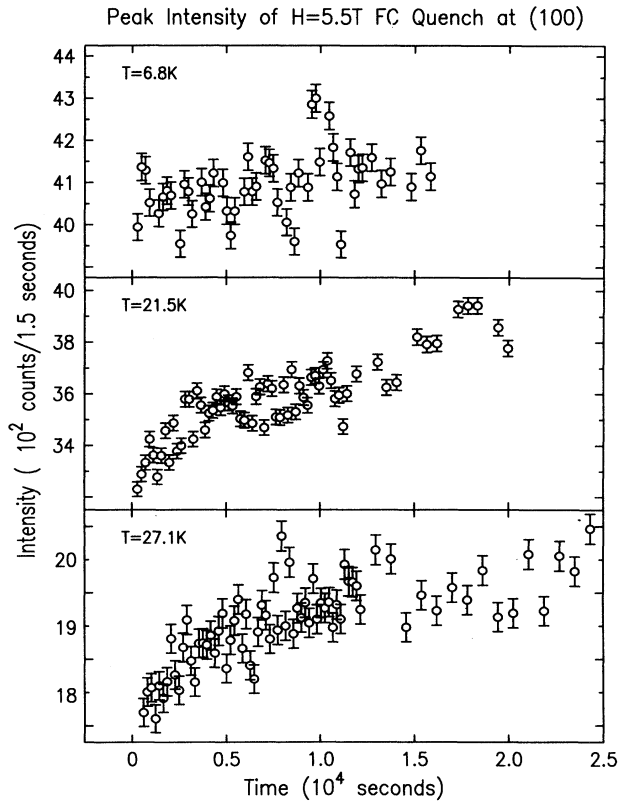


FIG. 1. The time dependence of the (100) magnetic peak intensity following FC quenches at  $H=5.5$  T to three temperatures  $T=6.8$  K (top panel),  $T=21.5$  K (middle panel), and  $T=27.1$  K (bottom panel). There is no detectable time dependence at  $T=6.8$  K, which is attributed to a freezing of the domain dynamics at low temperatures due to the Ising gap. At  $T=21.5$  K and  $T=27.1$  K, a pronounced increase in peak intensity is observed.

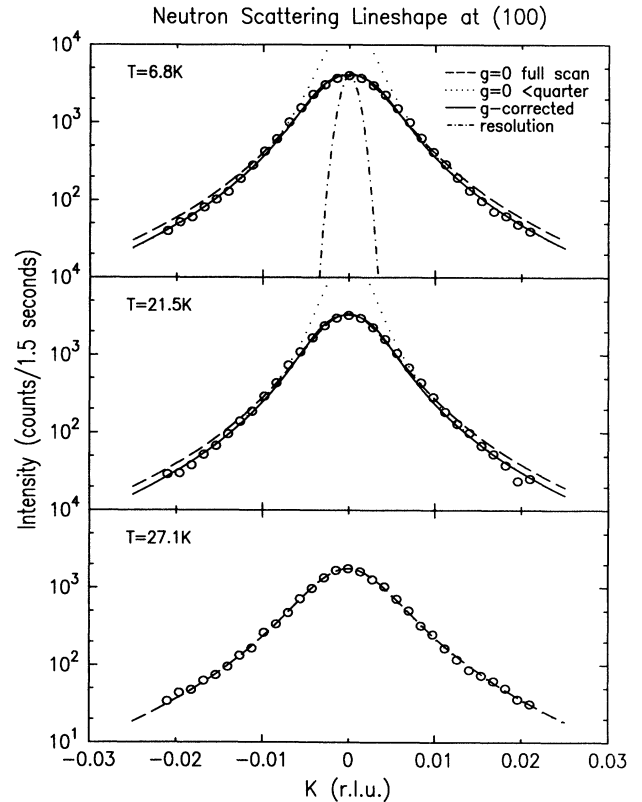


FIG. 2. Typical neutron-scattering transverse scans through the (100) Bragg peak during FC quenches to the temperatures  $T=6.8$  K ( $t=290$  s),  $T=21.5$  K ( $t=298$  s), and  $T=27.1$  K ( $t=605$  s) at  $H=5.5$  T. The solid lines show the extinction corrected fits at  $T=6.8$  and 21.5 K as discussed in the text. The dashed-lines represent fits to all data points and dotted-lines are fits to points below one quarter of the peak intensity, both without extinction correction. At  $T=27.1$  K, good fits were obtained without correction for extinction, and the fit to points below one quarter of the peak intensity is essentially identical to the fit to the full scan.

the wings. This cannot be attributed to the absence of a dynamic Lorentzian term in the cross section that would account for thermal fluctuations. Such a term can only increase the large  $q^*$  intensity. Furthermore, the energy resolution of the triple-axis mode is sufficiently high as to make the experiment insensitive to these fluctuations. As discussed previously by Cowley and co-workers,<sup>8,16</sup> the deviations are due to extinction effects which are commonly observed in neutron-scattering experiments on nearly perfect crystals. The  $\kappa$ 's obtained from the fits at  $T=6.8$  and 21.5 K are then in fact overestimates of the intrinsic widths. Therefore, these scans were refitted using only points that were below one third or one quarter of the peak intensity, since extinction effects were expected to be much smaller for these data points. The  $\kappa$ 's obtained this way were 50% smaller than those obtained from the earlier fits, but they displayed similar time dependences. However, the maximum value of the fitted curve exceeded the measured peak intensity in the data by more than a factor of 5 as expected because of the pronounced effects of the extinction. To maintain satisfactory fits and at the same time to account for extinction, we introduced a simple correction formula for secondary extinction,<sup>28</sup>

$$I_c = \frac{I}{1+gI}, \quad (2)$$

where  $I_c$  is the corrected intensity,  $I$  is the result of Eq. (1) convolved with the instrumental resolution and  $g$  is an empirical extinction correction parameter.  $A$  is then held constant for all the scans of a given quench. Excellent fits were obtained at  $T=6.8$  and 21.5 K by varying  $g$  and  $\kappa$ . Figure 2 shows examples of typical scans with the associated fits at the three temperatures. Again,  $\kappa$  is constant at  $T=6.8$  K but has pronounced time dependence at  $T=21.5$  K (Fig. 3). We stress that the time dependence seen here is *not* an artifact of the fitting function used.  $g$  is constant over time at  $T=6.8$  K but decreases slightly with increasing time at  $T=21.5$  K. Note that Eq. (1) is adequate at  $T=27.1$  K, indicating the absence of extinction at this temperature due to thermal fluctuations near  $T_c$  ( $g=0$ , bottom panel, Fig. 2).

From these fits, we estimate the correlation lengths at these temperatures to be  $360 \pm 10$  Å at  $T=6.8$  K,  $420 \pm 15$  Å at  $T=21.5$  K and  $160 \pm 5$  Å at  $T=27.1$  K. The correlation length at  $T=6.8$  K is smaller than that at  $T=21.5$  K, in qualitative agreement with the expectation that domains attain smaller size for quenches to lower temperatures because the energy barriers are less easily overcome through thermal activation. At  $T=27.1$  K, within 0.8 K of  $T_c$ , the correlation length is less than one-half of that at  $T=6.8$  and 21.5 K because the ordering of spins is broken up by thermal fluctuations.

Theory for the dynamics of the RFIM following a quench from high temperature predicts that the typical domain radius expands logarithmically with time. In their model, Grinstein and Fernandez<sup>15</sup> show that

$$R(t) \approx \frac{2JT}{h^2} \ln \frac{t}{\tau}, \quad (3)$$

where  $J$  is the exchange energy,  $T$  is the temperature, and

$h$  is the root-mean-squared random field strength.  $\tau$  is a characteristic microscopic attempt time.<sup>12,21,29</sup> For  $\text{Fe}_{0.5}\text{Zn}_{0.5}\text{F}_2$ , we estimate  $\tau = \hbar/E = 7.7 \times 10^{-13}$  s, where  $E$  is derived from the (111) zone-boundary magnon energy of  $\text{FeF}_2$ .<sup>30,31</sup> For a DAFF, the FC domain expansion is modified to be some power of a logarithmic function, depending on how the activation energy scales with the characteristic length scale of the system at time  $t$  and temperature  $T$ .<sup>21,32</sup> With the assumption  $\kappa(t) \sim R(t)^{-1}$ , we fit  $\kappa$  vs  $t$  to the following equation:

$$\kappa(t) = c \left( \ln \frac{t}{\tau} \right)^{-\psi_\kappa} \quad (4)$$

with  $\tau$  fixed at the value  $7.7 \times 10^{-13}$  s. For the quenches at  $T=21.5$  and 27.1 K, we obtain  $\psi_\kappa = 0.9 \pm 0.4$  and  $0.74 \pm 0.3$ , respectively. They are both compatible with a pure logarithmic decay and are within the range of estimates given by Huse and Henley<sup>33</sup> and Fisher,<sup>10</sup> but differ from the calculated value of 1.82 in Ref. 32. Equation (4) gives the solid lines shown in Fig. 3.

At  $T=6.8$  K, the inverse correlation length does not change with time. This is in agreement with the freezing of the dynamics at low temperatures observed by others and is attributed to the nonzero Ising excitation energy gap.<sup>19</sup>

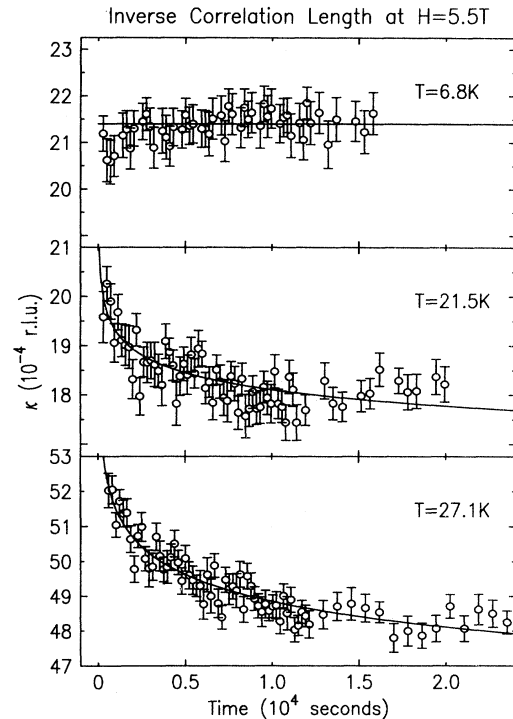


FIG. 3. Time dependence of the inverse correlation length  $\kappa$  obtained from fits such as those in Fig. 2. The growth of the FC domains at  $T=21.5$  and 27.1 K is illustrated. The domain size does not change at  $T=6.8$  K.  $\kappa$  at  $T=6.8$  and 21.5 K are obtained from extinction-corrected fits. The solid lines are best fits to Eq. (4) and show satisfactory agreement between the data and the logarithmic time dependence predicted by RFIM theory.

#### IV. SQUID MAGNETOMETRY RESULTS

Dynamics of  $2d$  and  $3d$  DAFF systems have been studied utilizing ac susceptibility,<sup>34</sup> optical Faraday rotation,<sup>18</sup> and SQUID magnetometry.<sup>19,22</sup> In particular, Lederman *et al.*<sup>19,22</sup> mapped out the dynamic behavior of  $\text{Fe}_{0.46}\text{Zn}_{0.54}\text{F}_2$  in the  $H$ - $T$  plane and related the decay of the uniform magnetization directly to the expansion of domains in the FC state. To complement the neutron work discussed above, we have carried out a similar series of SQUID measurements to study the FC domains in our crystal of  $\text{Fe}_{0.5}\text{Zn}_{0.5}\text{F}_2$ .

Temperature and field cycles of ZFC followed by FC and FH (heating the sample following a FC procedure in the same constant field) were performed at several fields between  $H = 0$  and 5.5 T to measure the uniform magnetization,  $M$ . Hysteresis was observed, showing sharp peaks in  $dM/dT$  following ZFC procedures but rounded and broadened peaks following FC or FH protocols. This is in qualitative agreement with other studies on strongly anisotropic DAFF's.<sup>18-20</sup> The sharp feature in  $dM/dT$  is now believed<sup>25</sup> to arise from a term in  $dM/dT$  that scales like  $dM_s^2/dT$ . During a ZFC run, the sample has achieved LRO so that the staggered magnetization  $M_s$  is nonzero and in a field a volume magnetization  $M_{\text{ZFC}}$  is also present. In the FC state, one expects an additional contribution to  $M$  from the domain walls. Following Lederman *et al.*,<sup>19</sup> we have subtracted  $M_{\text{ZFC}}$  from the FC magnetization  $M_{\text{FC}}$  at the corresponding temperature and thus obtained the excess magnetization  $M_{\text{ex}} = M_{\text{FC}} - M_{\text{ZFC}}$  which is believed to arise primarily from the domain walls. It is  $M_{\text{ex}}$  that may provide information about the size and the fractal properties of the magnetic domains. Figures 4 and 5 show  $M_{\text{ex}}$  vs  $t$  obtained from quenches taken at  $H = 1.5, 2.5, 3.45, 4, 5,$  and  $5.5$  T. In all cases, except for quenches to low temperatures ( $T \leq 15$  K), a significant decrease in  $M_{\text{ex}}$  is observed. At low temperatures,  $M_{\text{ex}}$  remains unchanged for at least 6 h to within experimental error for all the fields studied, in agreement with the frozen-spin picture.

In some previous reports on measurements of excess magnetization, the formula  $M_{\text{ex}}(t) \sim [\ln(t/\tau)]^{-1}$  has been applied to fit the data.<sup>18</sup> This assumes  $M_{\text{ex}}(t) \sim R(t)^{-1}$  and  $R(t)$  is given by Eq. (3), which is plausible if the domains are compact. However, these fits required unphysical values of  $\tau$ . Numerous simulation studies<sup>13,27,35</sup> have shown that the compact domain assumption is in fact unrealistic and domains in a strongly anisotropic DAFF form extremely complicated structures on all length scales. We find that only the  $M_{\text{ex}}$  decay at  $H = 3.45$  T agrees with this form satisfactorily. For the other fields,  $M_{\text{ex}}(t)$  does not follow a simple inverse logarithmic form.

Nattermann and Vilfan predicted that the time dependence of the magnetization arising from domain surfaces is given by<sup>21</sup>

$$M_s(t) \sim R^{-1} \left( \frac{T}{J} \ln \frac{t}{\tau} \right)^{-\psi_{\text{NV}}}. \quad (5)$$

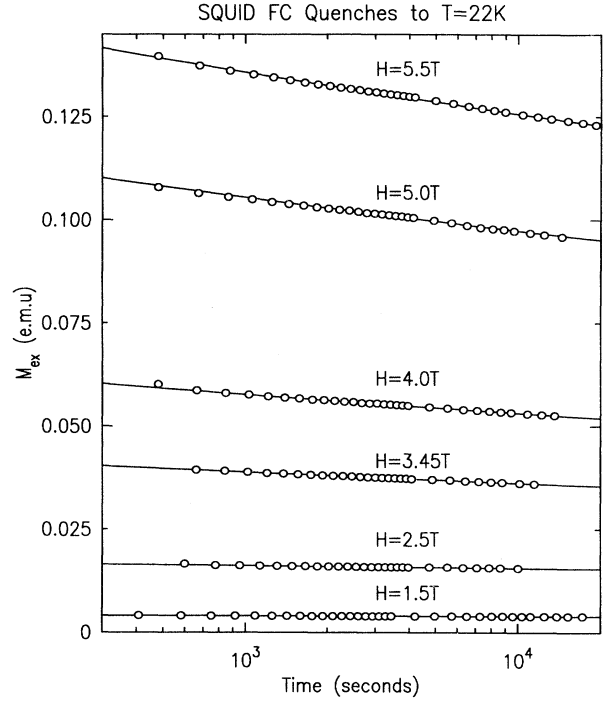


FIG. 4. Time dependence of quenched excess magnetization  $M_{\text{ex}}$  as measured by a SQUID magnetometer for  $T = 22$  K, at various fields. The solid lines are fits to Eq. (6) as discussed in the text. For  $H = 1.5$  and  $2.5$  T, the change in  $M_{\text{ex}}$  occurs within the first few points and the overall change is small compared to that at higher fields.

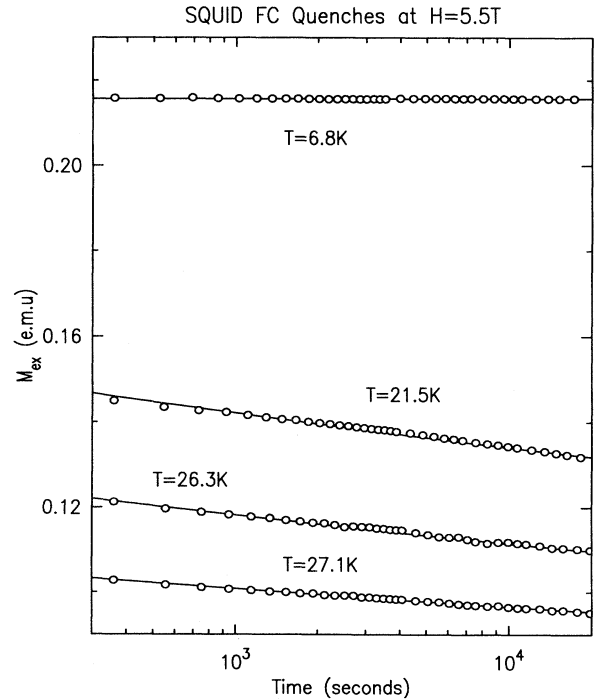


FIG. 5. Time dependence of the quenched excess magnetization  $M_{\text{ex}}$  as measured by the SQUID at various temperatures at  $H = 5.5$  T. The solid lines are fits to Eq. (6).  $M_{\text{ex}}$  is constant over time at  $T = 6.8$  K due to the finite Ising excitation gap at low temperatures.  $T_c(5.5 \text{ T}) = 27.9$  K.

The domain radius  $R \sim H^{\nu_M}$  and  $\nu_M = 2$  according to NV. The exponent  $\psi_{NV}$  is related to the fractal dimension of the FC domains.

Following Eq. (5), we fit our SQUID quench data to the form,

$$M_{ex} = c \left( \ln \frac{t}{\tau} \right)^{-\psi} \quad (6)$$

By varying the amplitude  $c$  and the exponent  $\psi$ , with  $\tau$  held fixed at  $7.7 \times 10^{-13}$  s, excellent fits were obtained and are shown as the solid lines in Figs. 4 and 5. We find that for a fixed temperature,  $\psi$  is field dependent. At  $T=22$  K,  $\psi(1.5 \text{ T})=0.42 \pm 0.14$ ,  $\psi(2.5 \text{ T})=0.58 \pm 0.06$ ,  $\psi(3.45 \text{ T})=1.10 \pm 0.03$ ,  $\psi(4 \text{ T})=1.26 \pm 0.05$ ,  $\psi(5 \text{ T})=1.24 \pm 0.08$ , and  $\psi(5.5 \text{ T})=1.20 \pm 0.05$ . Note that although  $\psi$  is much smaller than 1 at lower fields ( $H \leq 2.5$  T), its value does not vary much for fields above 3.45 T.

There is also some indication that the value of  $\psi$  is dependent upon the target temperature for quenches at a given field. For instance, at  $H=3.45$  T for which  $T_c=32.0$  K,  $\psi(22 \text{ K})=1.10 \pm 0.03$ , and  $\psi(30 \text{ K})=0.88 \pm 0.11$ . At  $H=5.5$  T from a later experiment on the same sample,  $\psi(21.5 \text{ K})=0.91 \pm 0.09$ ,  $\psi(26.3 \text{ K})=0.91 \pm 0.09$ , while  $\psi(27.1 \text{ K})=0.68 \pm 0.04$ . These results indicate that  $\psi$  becomes smaller as  $T_c$  is approached. In other words, near the transition temperature, the relative decrease in  $M_{ex}$  occurs at a slower rate. In all likelihood this is related to the anomalously slow relaxation in the critical region<sup>19</sup> arising from the activated dynamics, as proposed by Villain<sup>11</sup> and Fisher.<sup>10</sup> Further, the relative decay rate of  $M_{ex}$ , and therefore the value of  $\psi$ , depends on the rate of cooling during a quench. The smaller value of  $\psi(21.5 \text{ K})$  in the second run [compared to  $\psi(22 \text{ K})$  above] is due to such effect. The value of  $\psi$  has been measured previously in other experiments and its field and temperature dependence is consistent with the above observations.<sup>17</sup>

In order to investigate the scaling of the excess magnetization with the strength of the applied field, we extract from the quench data  $M_{ex}(T=22 \text{ K}) \sim H^{\nu_M}$  for the above six fields (Fig. 6) and obtain  $\nu_M=2.70 \pm 0.06$  at  $t=600$  s,  $\nu_M=2.69 \pm 0.04$  at  $t=3000$  s, and  $\nu_M=2.65 \pm 0.06$  at  $t=10000$  s. Therefore we estimate  $M_{ex} \sim H^{2.7+0.1}$  at all times. We discuss the significance of this power-law behavior in the next section.

Short quenches to various target temperatures were performed at  $H=5.5$  T. The magnetization measured at  $t=893$  s is shown in Fig. 7. Clearly, quenches to lower temperatures produce larger excess magnetization. Such temperature dependences agree qualitatively with the NV theory, but the predicted variation  $M_{ex} \sim T^{-\psi_{NV}}$  (Ref. 21) is not seen. This is not surprising in light of the fact that  $\psi$  is itself temperature dependent. The temperature dependence of  $\psi$  complicates the measurements because in practice quenching to a certain temperature cannot be instantaneous. Cooling through intermediate temperatures and the corresponding finite time interval both allow certain relaxation of the domains before the system reaches the target temperature. Thus one would expect that the observed quenched  $M_{ex}$  would deviate increas-

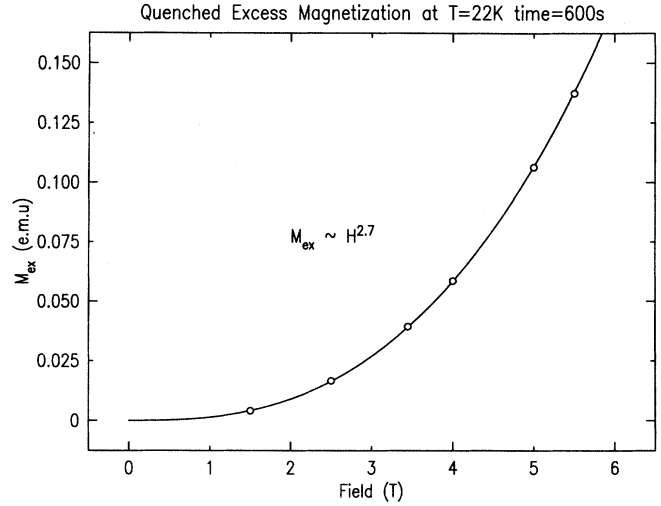


FIG. 6. The variation of quenched excess magnetization  $M_{ex}$  with respect to applied field  $H$  at  $T=22$  K,  $t=600$  s. This scaling differs from that of the FC inverse correlation length with field, as measured by neutron scattering, suggesting that the domains are fractal in nature.

ingly from an ideal  $T^{-\psi_{NV}}$  form at lower temperatures. This is obvious in Fig. 7. Instead of the  $T^{-\psi_{NV}}$  form, which diverges as  $T$  tends to zero,  $M_{ex}$  approaches a finite value at low temperatures. Compared to the quenched  $M_{ex}$ , the FC  $M_{ex}$  is substantially smaller in value and shows less dependence on temperature below

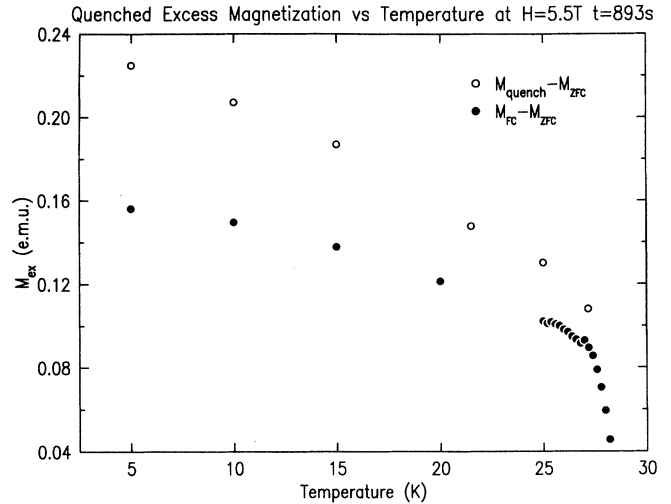


FIG. 7. The open circles show the excess magnetization  $M_{ex}$  as measured by SQUID following quenches to various temperatures below the transition at  $H=5.5$  T,  $t=893$  s. Quenches to lower temperatures produce larger  $M_{ex}$ . The results agree qualitatively with DAFF theory. The closed circles are excess magnetization measured in a gradual FC procedure. The difference between the quenched  $M_{ex}$  and the slow FC  $M_{ex}$  indicates the differing underlying domain structures formed during the two processes.

$T_c$ . The FC measurements are taken at a series of temperatures as the system is gradually cooled; this procedure clearly differs significantly from a rapid quench. Simulation studies have shown that there is no correspondence between the domains created during a quench and those formed during FC to the same temperature at the same field.<sup>13</sup>

## V. DISCUSSION

In a quenched DAFF system, the metastable domains expand through repositioning of the domain walls. Small, unfavorable domains are eliminated as the larger ones grow. From the parameters  $\tau$ ,  $J$ ,  $T$ , and an assumed fractal dimensionality  $D$ , we can estimate the length scale  $L$  on which energy barriers  $\Delta E \sim JL^D$  are overcome at a certain time  $t$ . At the time scale of our experiments on  $\text{Fe}_{0.5}\text{Zn}_{0.5}\text{F}_2$ ,  $L \sim a[(T/J)\ln(t/\tau)]^{1/D} \sim 25 \text{ \AA}$  at  $T=22 \text{ K}$ , where  $a=4.7 \text{ \AA}$  is the lattice constant in the plane perpendicular to the easy axis in  $\text{Fe}_{0.5}\text{Zn}_{0.5}\text{F}_2$  and  $D=2.5$  is assumed.<sup>35</sup>

A striking result from the magnetometry studies is the drastically different time-dependent behavior observed at low and high applied fields. For a low external field, for example,  $H \leq 1.5 \text{ T}$ , random bonds appear to play an important role in controlling domain formation.<sup>21</sup> Domains attain a relatively large size ( $R \sim 1600 \text{ \AA}$  at  $H=1.5 \text{ T}$ ) and a large part of the domain walls coincides with the boundary between magnetic and nonmagnetic ions, and is therefore pinned by RB's. Apparently the length scales on which domain surface adjustments occur are much smaller than the domain sizes. Hence a significant increase in the average domain size over time is not expected and the low-field situation falls into the regime of the NV theory which assumes a constant domain radius  $R$  and attributes any increase in the uniform magnetization to local readjustments in the domain surfaces. This implies that  $\psi$  measured at low fields by the SQUID experiment should be close to  $\psi_{\text{NV}} \approx 0.4$  for  $3d$  systems, and is evinced by our result at  $H=1.5 \text{ T}$ .

The smaller values of  $\psi$  for  $H \leq 2.5 \text{ T}$  reflect the smaller decrease of  $M_{\text{ex}}$  during quenches at these fields. This result agrees with the observation of Lederman *et al.*<sup>19,22</sup> who suggested that below a threshold field, the evolution of a DAFF system is controlled by random exchange dynamics, because the random-field pinning force is weak and the system relaxes significantly before a measurement can be made on a typical experimental time scale. For related work at low temperatures,  $T=2.8 \text{ K}$ , see Ref. 36.

The results in higher fields differ notably from those at lower fields. From the SQUID data, we estimate  $\psi=1.1 \pm 0.3$  for fields greater than  $H=3.45 \text{ T}$  and temperature above the region of frozen Ising dynamics. In this range of higher fields, the pinning force on the domain walls is derived from both RF's and RB's. Random-field dynamics now play a significant role in the evolution of domains. This is evidenced by scattering experiments which show a significant increase in domain radii when the external field is decreased (though the system remains in a SRO state).<sup>8,23</sup> The length scales  $L$ , on which the domain walls shift are no longer negligible

compared to the correlation length according to our neutron-scattering results. The average size of the domains increases notably over time. For example, the change in correlation length  $\Delta\xi$  at  $T=21.5 \text{ K}$  and  $H=5.5 \text{ T}$  is approximately  $40 \text{ \AA}$  during the 5 h time span of the neutron-scattering measurements. This may be compared with  $L \sim 25 \text{ \AA}$  estimated above. It is interesting to note that  $\Delta\xi$  and  $L$  are of comparable magnitude.

The domain relaxation has a direct effect on the excess uniform magnetization  $M_{\text{ex}}$ . In Fig. 8, we show a comparison of the inverse correlation length  $\kappa$  obtained from fits of the neutron scattering data and the rescaled  $M_{\text{ex}}$  determined by SQUID measurements, taken at the same temperatures at  $H=5.5 \text{ T}$ . At  $T=6.8 \text{ K}$ , both techniques show that the magnetic domains are frozen. At  $T=21.5$  and  $27.1 \text{ K}$ ,  $\kappa$  and  $M_{\text{ex}}$  undergo a similar percentage of decay over the same period of time. The agreement is also reflected in the fact that  $\psi_\kappa$  obtained from neutron scattering and the  $\psi$  from the SQUID data are equal to within the combined errors. In this high-field regime, our results are compatible with the assumption  $M_{\text{ex}}(t) \sim \kappa(t)$  made by others.<sup>19</sup> One might also im-

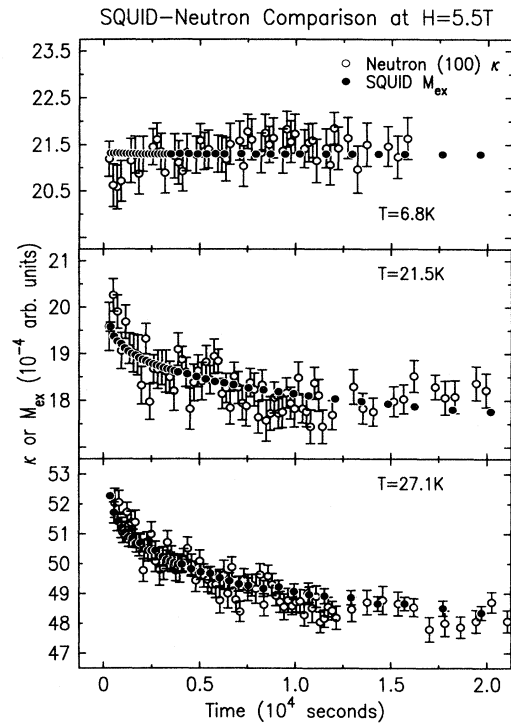


FIG. 8. Comparison of the time dependence of the inverse correlation length  $\kappa$ , as measured by neutron scattering and the excess magnetization from domain walls  $M_{\text{ex}}$  as measured by the SQUID for three temperatures below the transition. The  $M_{\text{ex}}$  values have been rescaled according to the neutron scattering  $\kappa$ . Both techniques show frozen dynamics at low temperatures. At higher temperatures, the two techniques also agree, suggesting that the fractal properties of the domains do not change noticeably while the average size of the domains grow with time.

agine a scenario in which the time dependence seen in  $M_{\text{ex}}$  arises from both an overall domain growth and local adjustments in domain walls. Assuming neutron scattering is sensitive to the former effect but not the latter, one would then expect  $\psi = \psi_{\kappa} + \psi_{\text{NV}} \approx (0.9 \pm 0.4) + 0.4 = 1.3 \pm 0.4$ . Although this does not conflict with our fitted values for  $\psi$  in high fields, this scenario is probably invalid because in deriving Eq. (5), NV assume a well defined domain of time-independent radius  $R$  that is compact on large length scales. In fact, simulations have suggested that domain walls are fractal for DAFF's in strong dilution and applied fields.<sup>27</sup> Therefore, the agreement between the time dependence of our  $\kappa(T)$  and  $M_{\text{ex}}(T)$  suggests that the neutron scattering and the SQUID magnetometry techniques observe the same time-dependent effects in  $\text{Fe}_{0.5}\text{Zn}_{0.5}\text{F}_2$ . The higher value of  $\psi$  at fields  $H \geq 3.45$  T is clearly a random-field effect and should therefore be distinguished from the behavior for  $H \leq 1.5$  T. The magnetometry results at  $H = 2.5$  T lie between these two regimes.

We next turn to a discussion of the field dependence of the excess magnetization. Instead of  $M_{\text{ex}} \sim H^2$  as predicted by theory,<sup>21</sup> we find  $M \sim H^{\nu_M}$  with the exponent  $\nu_M = 2.7 \pm 0.1$ , which is somewhat smaller than the  $3.2 \pm 0.3$  reported by Lederman *et al.*<sup>22</sup> Because the FC domains are fractal,  $\nu_M$  need not be the same as the exponent  $\nu_H$  which describes the scaling of the inverse correlation length with the magnetic field,  $\kappa \sim H^{\nu_H}$ , as measured by neutron-scattering experiments. Cowley *et al.* obtained  $\nu_H = 2.2 \pm 0.1$  in  $\text{Fe}_{0.5}\text{Zn}_{0.5}\text{F}_2$ .<sup>8</sup>

The fact that  $\nu_M$  is larger than  $\nu_H$  may be understood by considering the disordered nature of the domain walls. As the external field increases, the local random-field increases proportionally, the RF pinning force is therefore stronger and hence the domain interface is generally rougher and more entangled, adding an extra surface magnetization contribution to the simple increase of  $M_{\text{ex}}$  due to the smaller domain size in higher fields.

Numerical studies of the kinetics of  $3d$  RFIM domain growth show that the early-time expansion follows the Lifshitz-Cahn-Allen law  $R(t) \sim t^{1/2}$  which subsequently evolves into an asymptotic logarithmic behavior only after a field-dependent crossover time.<sup>32,37</sup> This crossover is not seen in either the neutron or the SQUID measurements, presumably because it happens much before the first quench datum point is taken in either case.

This work and others<sup>22</sup> have shown that the metastable

state of a FC DAFF is dependent not only upon the history of this state but also the time scale it is probed on. The evolution of the domains contributes to the hysteresis seen in the various measurements on all metastable RFIM systems. One example is the fact that the FH  $dM/dT$  peak is generally sharper than the FC peak at the same field (above a certain threshold field in  $\text{Fe}_x\text{Zn}_{1-x}\text{F}_2$ ) in bulk measurements.<sup>18,22</sup>

## VI. SUMMARY

We have performed a comparative neutron-scattering and SQUID magnetometry study of the time-dependent magnetic domain morphology in the quenched FC states of strongly anisotropic DAFF's. Our neutron-scattering data at  $H = 5.5$  T provide direct evidence of logarithmic domain growth. SQUID magnetometry gives dramatically different results at high and low applied fields and suggests that the relevant time-dependent effects are governed by different dynamics. At high fields, the inverse domain size  $\kappa$  and the excess magnetization  $M_{\text{ex}} = M_{\text{FC}} - M_{\text{ZFC}}$  exhibit closely similar time dependences at temperatures  $T \ll T_c(H)$ ,  $T \sim 0.7T_c(H)$ , and  $T \sim T_c(H)$ . This demonstrates that, to first order at least, the excess FC magnetization resides in the domain walls. The study of the formation and dynamics of the domain state is crucial to the understanding of how DAFF's behave in a complex free-energy landscape created by RF's and RB's. We hope that further study on these phenomena, both experimentally and theoretically, will yield a more detailed and consistent physical description of domains in DAFF's with quantitative values for the important exponents.

## ACKNOWLEDGMENTS

We thank T. R. Thurston for his valuable assistance on the neutron-scattering experiments. We also thank Arlette Cassanho for growing the excellent  $\text{Fe}_{0.5}\text{Zn}_{0.5}\text{F}_2$  crystals studied here. The work at MIT was supported by the National Science Foundation under Grant No. DMR-9315715, and in part by the MRSEC Program of the National Science Foundation under Grant No. DMR-9400334. The work at Brookhaven National Laboratory was carried out under Contract No. DE-AC02-76CH00016, Division of Materials Science, U.S. Department of Energy.

<sup>1</sup>R. J. Birgeneau, Y. Shapira, G. Shirane, R. A. Cowley, and H. Yoshizawa, *Physica* **137B**, 83 (1986).

<sup>2</sup>T. Nattermann and J. Villain, *Phase Transitions* **11**, 5 (1988).

<sup>3</sup>Y. Imry and S.-K. Ma, *Phys. Rev. Lett.* **37**, 1399 (1975).

<sup>4</sup>J. Z. Imbrie, *Phys. Rev. Lett.* **53**, 1747 (1984).

<sup>5</sup>S. Fishman and A. Aharony, *J. Phys. C* **12**, L729 (1979).

<sup>6</sup>J. L. Cardy, *Phys. Rev. B* **29**, 505 (1984).

<sup>7</sup>P. Wong and J. W. Cable, *Phys. Rev. B* **28**, 5361 (1983).

<sup>8</sup>R. A. Cowley, H. Yoshizawa, G. Shirane, and R. J. Birgeneau, *Z. Phys. B* **58**, 15 (1984).

<sup>9</sup>Y. Shapira, N. F. Oliveira, Jr., and S. Foner, *Phys. Rev. B* **30**, 6639 (1984).

<sup>10</sup>D. S. Fisher, *Phys. Rev. Lett.* **56**, 416 (1986).

<sup>11</sup>J. Villain, *J. Phys. (Paris)* **46**, 1843 (1985).

<sup>12</sup>J. Villain, *Phys. Rev. Lett.* **52**, 1543 (1984).

<sup>13</sup>G. S. Grest, C. M. Soukoulis, and K. Levin, *Phys. Rev. B* **33**,

- 7659 (1986).
- <sup>14</sup>J. P. Hill, Q. Feng, R. J. Birgeneau, and T. R. Thurston, *Z. Phys. B* **92**, 285 (1993).
- <sup>15</sup>G. Grinstein and J. F. Fernandez, *Phys. Rev. B* **29**, 6389 (1984).
- <sup>16</sup>R. A. Cowley, G. Shirane, H. Yoshizawa, Y. J. Uemura, and R. J. Birgeneau, *Z. Phys. B* **75**, 303 (1989).
- <sup>17</sup>S.-J. Han, D. P. Belanger, W. Kleemann, and U. Nowak, *Phys. Rev. B* **45**, 9728 (1992).
- <sup>18</sup>P. Pollak, W. Kleemann, and D. P. Belanger, *Phys. Rev. B* **38**, 4773 (1988).
- <sup>19</sup>M. Lederman, J. V. Selinger, R. Bruinsma, J. Hammann, and R. Orbach, *Phys. Rev. Lett.* **68**, 2086 (1992).
- <sup>20</sup>U. A. Leitão, W. Kleemann, and I. B. Ferreira, *Phys. Rev. B* **38**, 4765 (1988).
- <sup>21</sup>T. Nattermann and I. Vilfan, *Phys. Rev. Lett.* **61**, 223 (1988).
- <sup>22</sup>M. Lederman, J. V. Selinger, R. Bruinsma, R. Orbach, and J. Hammann, *Phys. Rev. B* **48**, 3810 (1993).
- <sup>23</sup>Q. Feng, Q. J. Harris, and R. J. Birgeneau (unpublished).
- <sup>24</sup>J. P. Hill, Q. Feng, R. J. Birgeneau, and T. R. Thurston, *Phys. Rev. Lett.* **70**, 3655 (1993).
- <sup>25</sup>R. J. Birgeneau, Q. Feng, Q. J. Harris, J. P. Hill, A. P. Ramirez, and T. R. Thurston (unpublished).
- <sup>26</sup>H. Yoshizawa, R. A. Cowley, G. Shirane, and R. J. Birgeneau, *Phys. Rev. B* **31**, 4548 (1985).
- <sup>27</sup>U. Nowak and K. D. Usadel, *Phys. Rev. B* **46**, 8329 (1992).
- <sup>28</sup>*Fundamentals of Crystallography*, edited by C. Giagovazzo (Oxford Science, Oxford, 1992).
- <sup>29</sup>J. Prejean and J. Souletie, *J. Phys. (Paris)* **41**, 1335 (1980).
- <sup>30</sup>M. T. Hutchings, B. D. Rainford, and H. J. Guggenheim, *J. Phys. C* **3**, 307 (1970).
- <sup>31</sup>R. J. Birgeneau, R. A. Cowley, G. Shirane, D. P. Belanger, A. R. King, and V. Jaccarino, *Phys. Rev. B* **27**, 6747 (1983).
- <sup>32</sup>Z. W. Lai, G. F. Mazenko, and O. T. Valls, *Phys. Rev. B* **37**, 9481 (1988).
- <sup>33</sup>D. A. Huse and C. L. Henley, *Phys. Rev. Lett* **54**, 2708 (1985).
- <sup>34</sup>A. G. Schins, A. F. M. Arts, and H. W. de Wijn, *Phys. Rev. Lett.* **70**, 2340 (1993).
- <sup>35</sup>J. L. Cambier and M. Nauenberg, *Phys. Rev. B* **34**, 7998 (1986).
- <sup>36</sup>J. Kushaer, W. Kleemann, J. Mattsson, and P. Nordblad, *Phys. Rev. B* **49**, 6346 (1994).
- <sup>37</sup>M. Rao and A. Chakrabarti, *Phys. Rev. Lett.* **71**, 3501 (1993).